

Electronic Supplementary Information

Lithiation/Delithiation of Silicon Heavily Doped with Boron Synthesized Using the Czochralski Process

^a Department of Materials Chemistry, Faculty of Engineering, Shinshu University

^b Technical Division, Faculty of Engineering, Shinshu University

^c Department of Electrical and Computer Engineering, Shinshu University

4-17-1 Wakasato, Nagano 380-8553, Japan

Masahiro Shimizu,^{a,*} Kohei Kimoto,^a Ayaka Kikuchi,^b
Toshinori Taishi,^c Susumu Arai^a

Dr. Masahiro Shimizu

Tel: +81-26-269-5627; Fax: +81-26-269-5432

E-mail: shimizu@shinshu-u.ac.jp

Table S1. Summary of undoped Si (11N) and B- and P-doped Si synthesized by a Czochralski method: dopant species, concentration, electrical conductivity, lattice constant, initial charge–discharge capacities, and Coulomb efficiency.

Sample	Dopant	Concentration / ppm (at.%) ^a	Atomic density / atoms cm ⁻³	Electrical conductivity / mΩ cm ^b	Lattice constant / Å ^c	1 st capacities / mA h g ⁻¹	1 st C.E. (%)
1)	- (11N)	Undoped	5.0×10^{22}	10^8	5.431	3364 / 3915	86
2)	P	2000 (0.20)	1.0×10^{20}	0.9	5.431	3389 / 3828	89
3)	B	300 (0.03)	1.5×10^{19}	6.5	5.429	3402 / 3943	86
4)	B	1600 (0.16)	8.0×10^{19}	1.6	5.428	3359 / 3920	86
5)	B	4700 (0.47)	2.4×10^{20}	0.6	5.425	3284 / 3786	87
6)	B	12400 (1.24)	6.2×10^{20}	0.3	5.415	2979 / 3622	82

a) ICP by an alkali fusion method.

b) Four-terminal type impedance measurement.

c) Estimated value from the dopant concentration (ref.1).

Ref.1) G. Masetti, M. Severi, S. Solmi, *IEEE Trans. Electron Devices*, **30** (1983) 764–769.

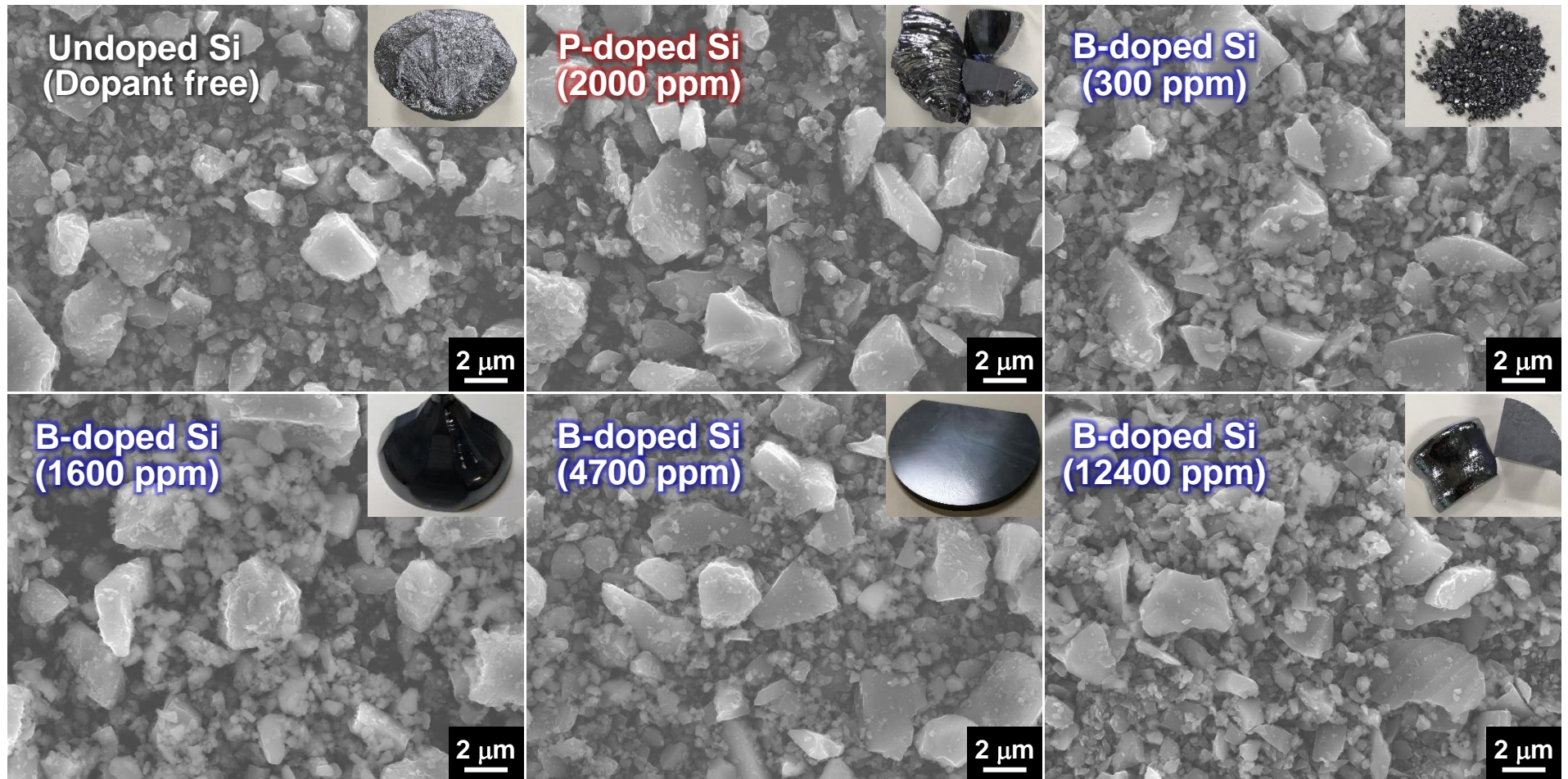


Figure S1. SEM images of 11N-Si (dopant free), P-doped Si (2000 ppm), B-doped Si (600, 1600, 4700, 12400 ppm) powders crushed by mechanical milling. Insets: Si ingots prepared by the Czochralski method (300 ppm-B doped Si: crushed granules). the 300 ppm-B doped Si was prepared from a diluted melt of the Si with highly concentrated B and polycrystalline Si.

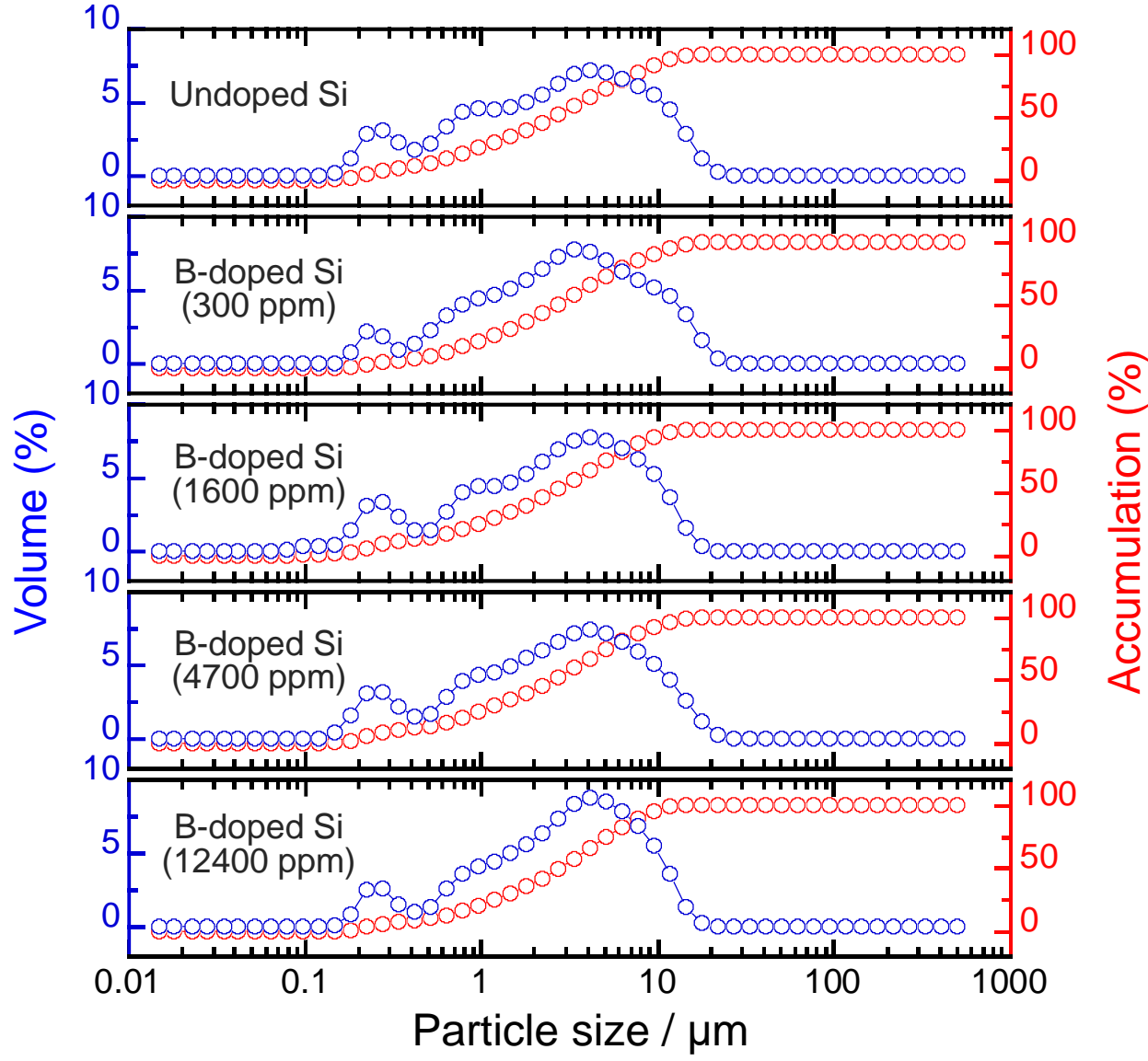


Figure S2. Particle size distributions of 11N-Si (dopant free) and B-doped Si (600, 1600, 4700, 12400 ppm) powders used in the preparation of mixture electrodes in this work. Ingots were fractured to granule size in a mortar prior to mechanical milling (MM). The respective MM times were set to keep the particle size distributions about the same.

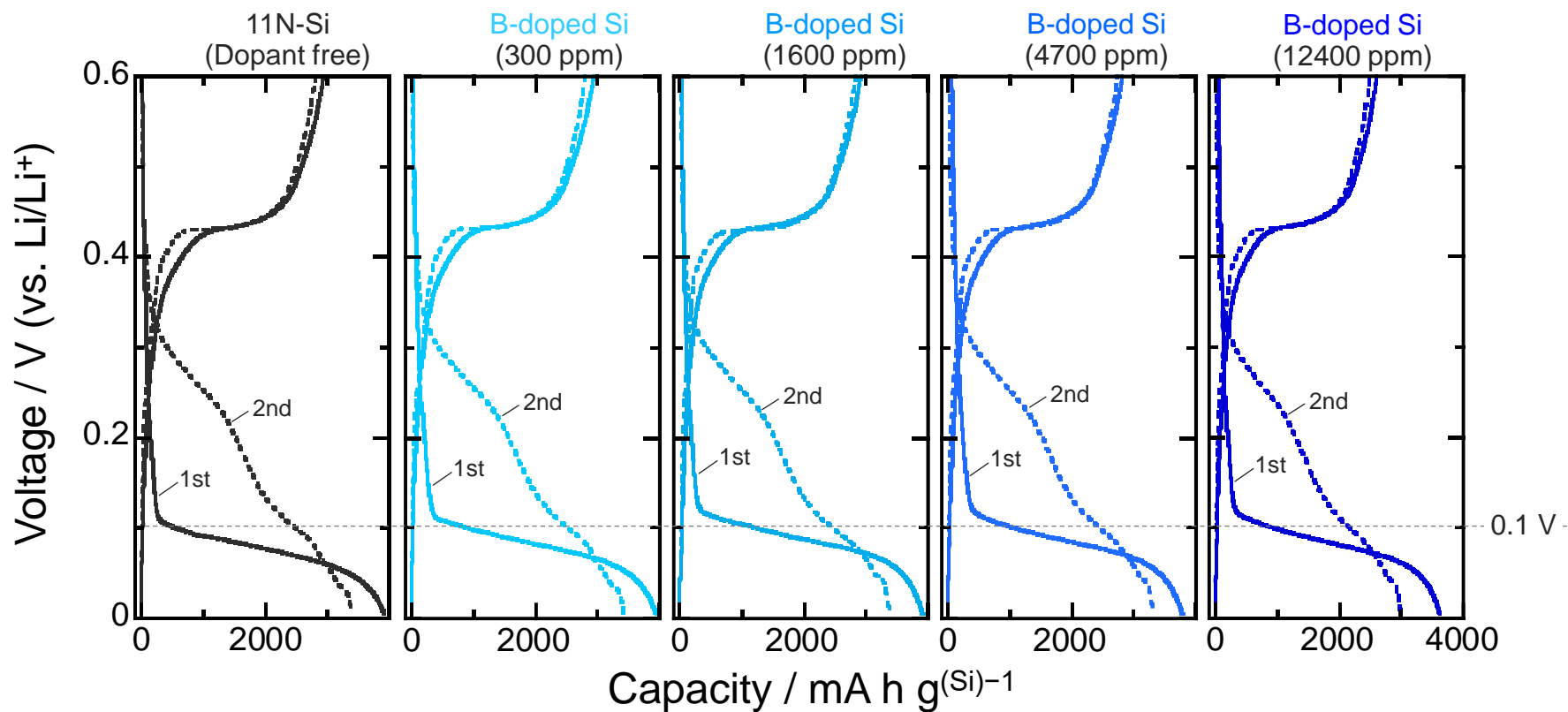


Figure S3. Enlarged view of galvanostatic charge–discharge curves (Figure 2a) of undoped (dopant free) and B-doped Si (600, 1600, 4700, and 12400 ppm) electrodes in 1 M $\text{LiPF}_6/\text{EC}:\text{DEC}$ (50:50 vol.%) at a current density of 358 mA g^{-1} ($0.1C$). The onset voltages of lithiation for the B-doped Si are higher than that of the undoped Si irrespective of B concentrations.

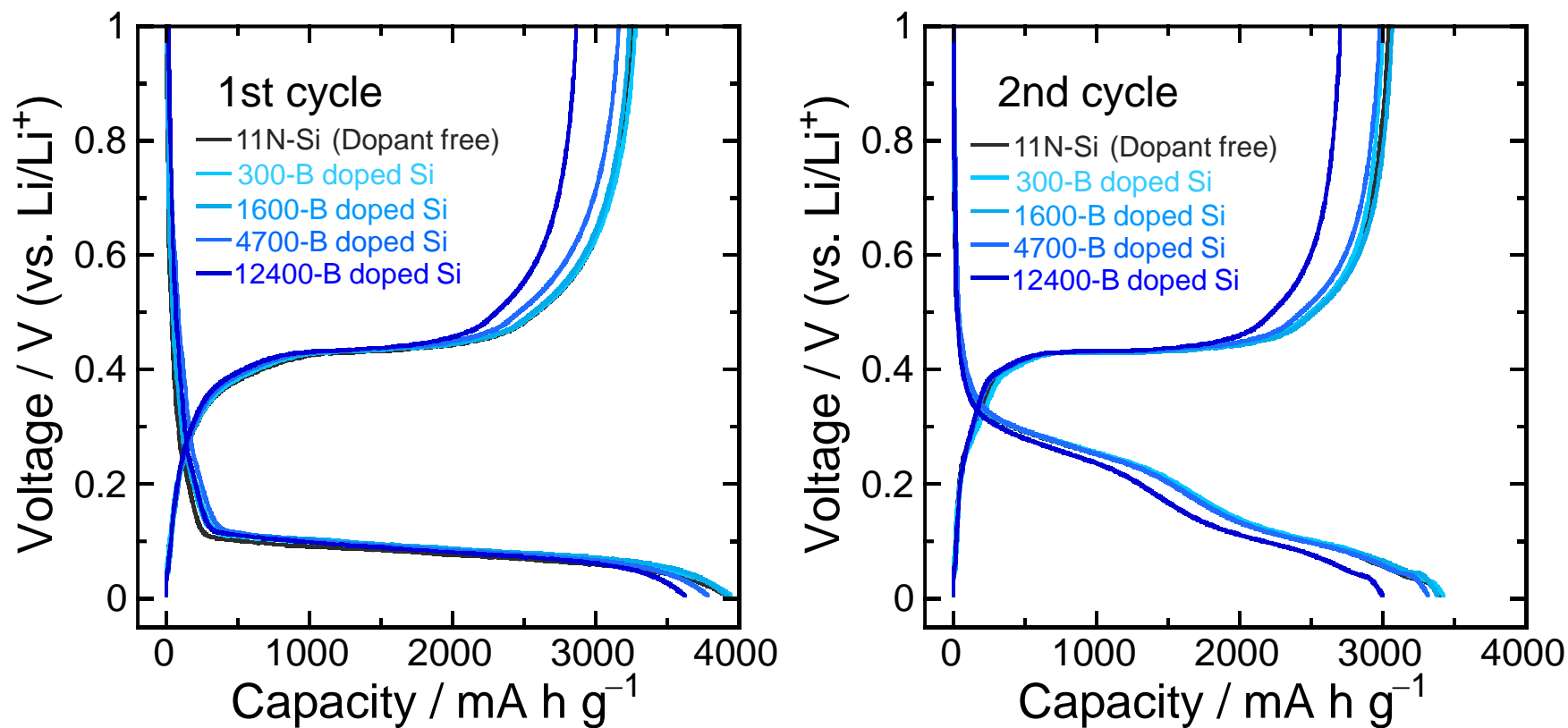


Figure S4. Comparison of first and second charge–discharge curves (Figure 2a) of undoped (dopant free) and B-doped Si (600, 1600, 4700, and 12400 ppm) electrodes in 1 M $\text{LiPF}_6/\text{EC}:\text{DEC}$ (50:50 vol.%) at a current density of 358 mA g^{-1} ($0.1C$). The onset voltages of lithiation for the B-doped Si are higher than that of the undoped Si irrespective of B concentrations.

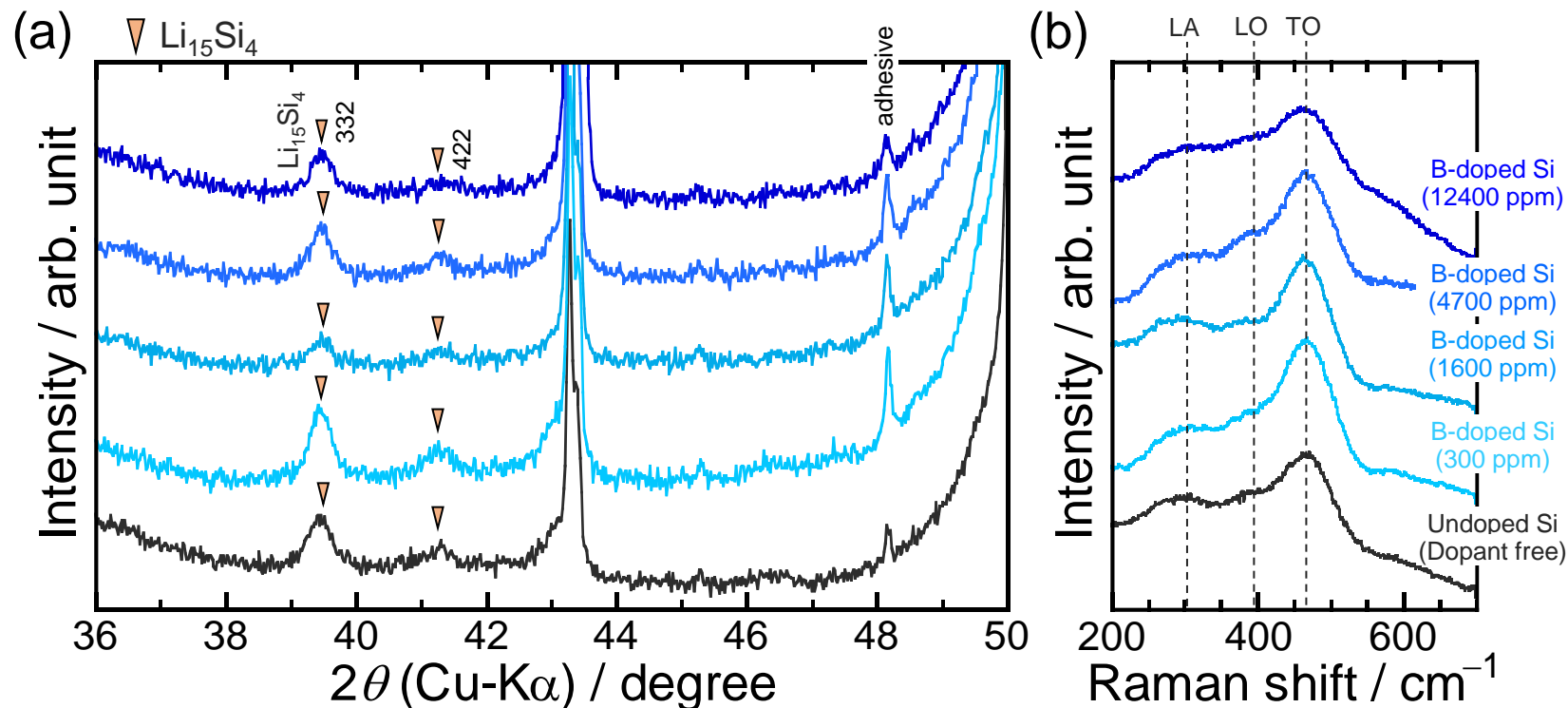


Figure S5. (a) XRD patterns of undoped Si and B-doped (300, 1600, 4700, 12400 ppm) Si electrodes at the lithiation voltage of 0.005 V (vs. Li/Li⁺). The electrodes were charged and discharged at a current density of 358 mA g⁻¹ (0.1C). (b) Raman spectra of undoped Si and B-doped Si electrodes after the first delithiation (upper cut-off voltage: 2.0 V). Crystalline Si undergoes amorphization after the first lithiation/delithiation process to transform into amorphous Si, which was observed from the Raman spectra. After the first cycle, the vibrations of Si–B (¹¹B, ¹⁰B) bonds were not detected.

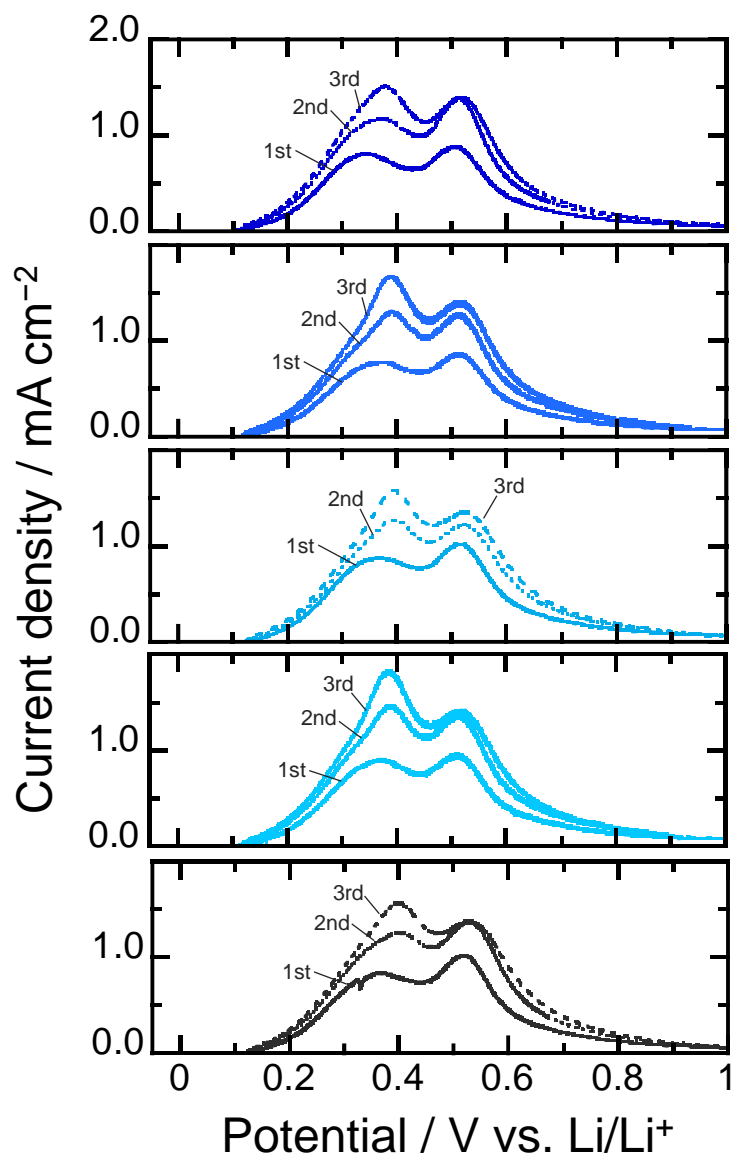
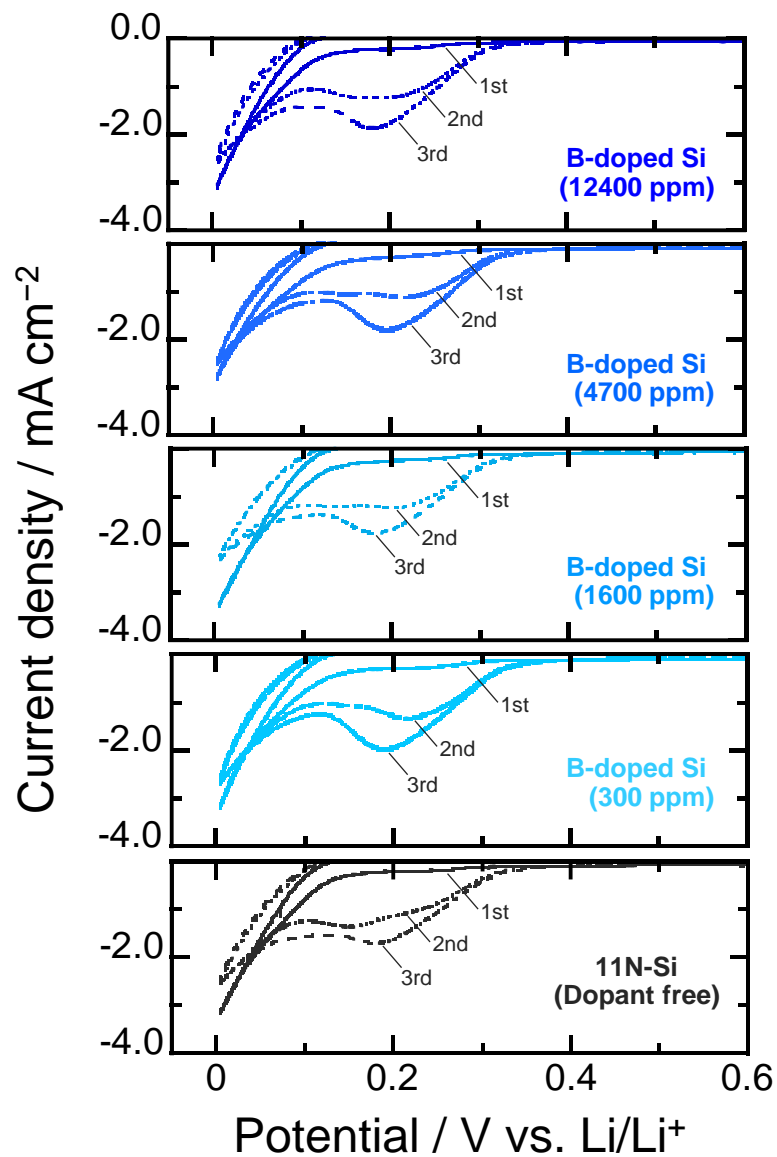


Figure S6. Cyclic voltammograms of undoped and B-doped Si (600, 1600, 4700, and 12400 ppm) electrodes in 1 M LiPF₆/EC:DEC (50:50 vol.%) at a sweep rate of 0.1 mV s⁻¹. Left: cathodic scan, Right: anodic scan.

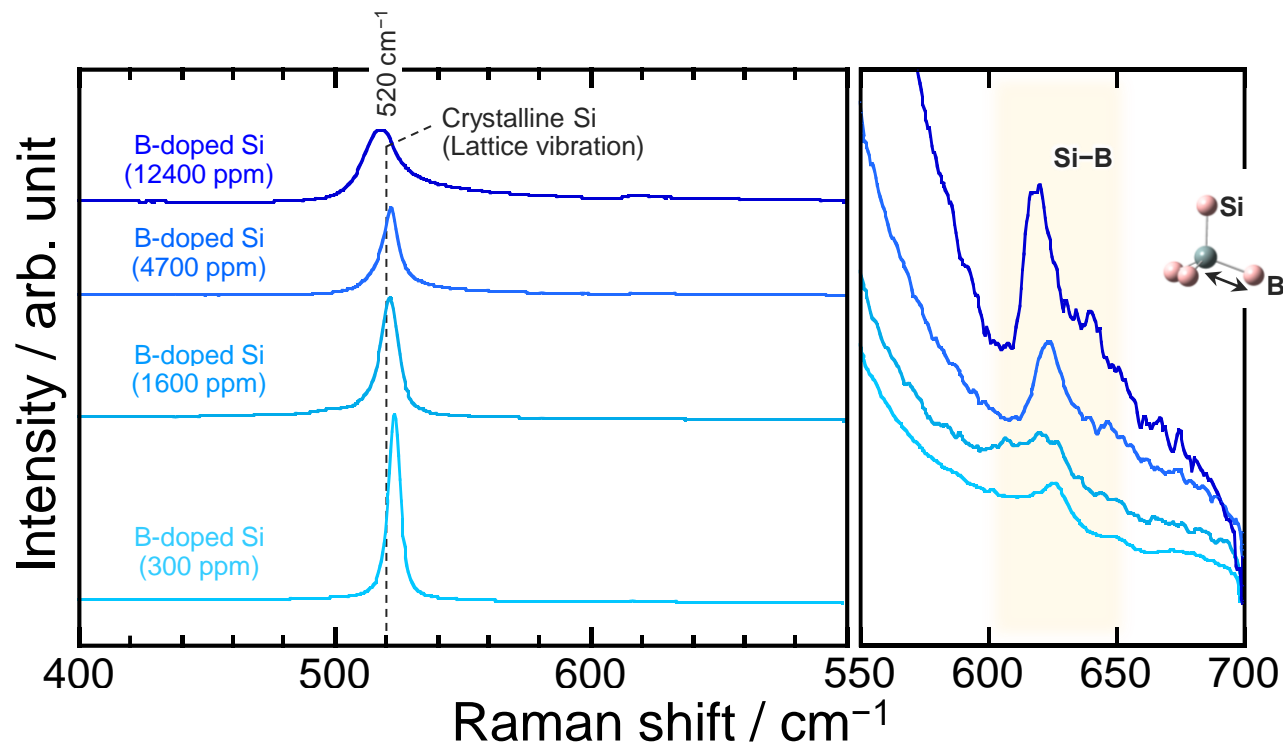


Figure S7. Raman spectra of undoped Si and B-doped Si electrodes crystallized by the laser irradiation (wavelength: 532 nm) for 30 min. The undoped Si and B-doped Si electrodes were charged and discharged for one cycle at a current density of 358 mA g⁻¹ (0.1C), which resulted in the amorphization of the Si and the B-doped Si. The vibrations of Si⁻¹¹B and Si⁻¹⁰B bonds were again detected. Therefore, even in the case of the pulverization and fracture of the active material due to the huge volume change in Si during lithiation/delithiation, the conductive network of the entire electrode structure is expected to be maintained.

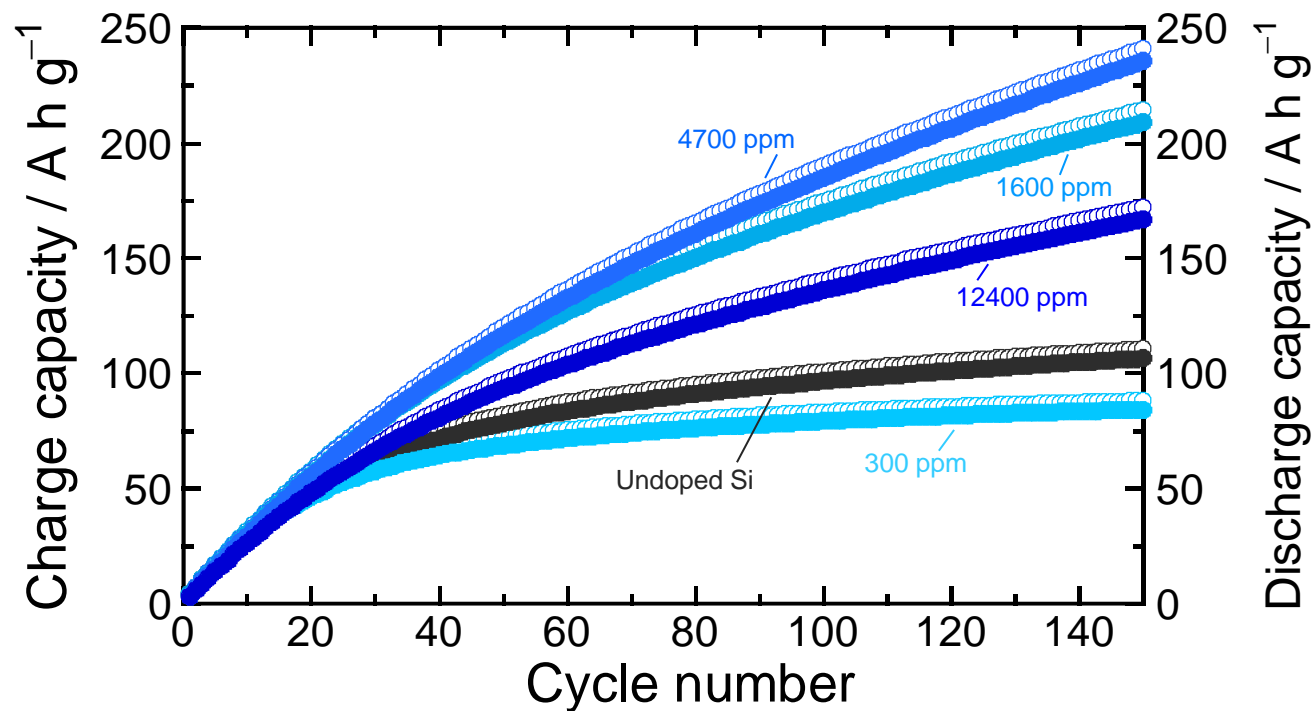


Figure S8. Dependence of integrated lithiation/delithiation capacity of B-doped Si electrodes under the galvanostatic condition with a current density of 358 mA g^{-1} ($0.1C$). The lithiation/delithiation capacities of at the 4700 ppm-B doped Si at the initial cycles are slightly smaller than those of the 1600 ppm-B doped Si, meaning that the degree of volume change is also relatively lower. The lower volume change appears to result in the better cycling performance, but rather, the 4700 ppm-B doped Si actually has larger integrated capacities after the 100 cycles.